A novel method for the reduction of switching operations of ULTC & SCs

.Dr.CHEN CHOU
EEE Department
GMR Institute of Technology, Rajam, AP, India
ramakrishna.r@gmrit.edu.in

PROF.S.M.PRASAD
EEE Department
CVR College of engineering
HYDERABAD, India
dakkaobulesh@gmail.com

Dr.REGAN MOODY
EEE Department
N B K R Institute of Science & Technology, *Nellore,* India
sankar.neeru@gmail.com

***Abstract*— the presence of dispatchable Distributed Generations (DDGs) is increasing recently on distribution systems. the presence of DDGs increasing the switching operations of Under Load Tap Changer (ULTC) and Shunt Capacitors (SCs). This leads to reduce the life of ULTC & SCs. Proper reactive power management is required among DDGs, ULTC and SCs to curtail switching operations and to enhance the life of switching devices (ULTC & SCs). This paper proposes a novel method for reactive power coordination, in which the loads are forecasted one day in advance and then the objective function is formulated as combination of Switching loss and power loss. The objective function is optimized using Particle Swarm Optimization (PSO) algorithm. The proposed method is designed and implemented in MATLAB/Simulink environment on 10kV, 16 bus system. The performance of proposed method is compared with conventional method. findings reported that proposed method is effective as compared with conventional without violating the grid conditions.**

Keywords*— Dispatchable Distributed Generation (DDG); SCs, ULTC.

I. INTRODUCTION

The use of distributed generation, often known as DG, has grown quickly in order to maintain acceptable levels of voltage and power loss in distribution systems. The efficiency of the distribution system and the reactive power-controlled devices (RPCDs) connected to it are both greatly impacted by the rising share of dispersed generation. This severely affects the lifespan of RPCDs such as ULTCs and shunt capacitors by increasing steady-state voltage fluctuations and switching operations (SOs) [1]. Controlling and coordinating the reactive power of DG with RPCDs enhances the efficiency of both the distribution system and the RPCDs. As a result, it has become a hot research topic [2]. Investigations [3-8] have been conducted on a wide range of methods to the formulation of coordination problems. Vivan and Karlsson [3] proposed a mixed local and distant voltage technique that used an induction machine as a DG to manage reactive power. This device functioned as a distributed generator. [4] suggests a method for managing voltage and reactive power that makes use of an under-load tap changer (ULTC), shunt capacitors, and a synchronous machine as a DG. An optimal power flow approach was proposed in reference to the challenge of coordinating reactive power from DG, ULTC, and SCs within a network while adhering to voltage step limits. [6] presents a strategy for managing ideal power flow based on increasing DG real power while taking network loss into account as a constraint. Sheng and colleagues [7] proposed trust region sequential quadratic programming to optimize resource utilization by coordinating with one-day-ahead projected load. To manage the steady-state voltage of the DG, ULTC, and SC, the Kim proposed Dynamic Programming Technique (DPM) should be utilized [8]. An innovative voltage control method for reducing voltage deviations was created by [9] by combining the reactive power of ULTC, SCs, and inverter-based DG. Voltage fluctuations would be lessened as a result. In [10], it was recommended to employ particle swarm optimization (PSO) as a coordinating mechanism, with the DG operating as a synchronous machine and load anticipated one day in advance. Particle Swarm Optimization (PSO) was proposed as a method for coordinating the dispatchable DG, ULTC, and SC in [11]. The improved search harmony (ISH) method, which is described in [12], was used to optimize the ULTC, SCs, and DG reactive power regulation problem. The DFIG wind system coordinated its operations with the ULTC and the SCs in [13–14] using the GWO technique.

Single dispatchable distributed generation (DDG) is the primary methodology discussed in the research literature, with non-dispatchable distributed generation (NDDG) receiving very little attention. In this paper, a coordination problem involving many DGs is first formulated. The Adaptive Neuro Fuzzy Inference System (ANFIS) approach is then utilized to anticipate the load hourly one day in advance. Finally, the coordination problem is optimized using the Particle Swarm Optimization (PSO) algorithm.

This paper is organized into five sections. First section is discussing about literature and second one is problem formulation. Implementation of proposed method discussed in section 3 and section 4 describes about test system and simulation results. Finally, conclusions based on findings are discuses in chapter 5.

II. PROBLEM FORMULATION

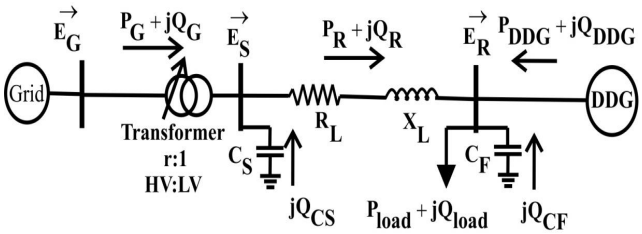

Fig.1(a). Grid connected system with DDG and DFIG.

In this paper, a simple radial distribution system is considered for problem formulation and is shown in Fig.1. The system operators decide the dispatched schedule of the active power of the DDG, and the grid conditions control the reactive power schedule of DDG. The ULTC is placed on the transformer's high voltage side, which controls the entire distribution feeder voltage. The SCs are placed at the receiving end and the sending end. These are

parallellyconnected group of unit capacitors with individual control. ULTC and SCs control the distribution feeder voltages up to a small percentage of rated value; therefore, the DDG can absorb or supply the required reactive power amount. For the numerical simplification, the power loss in the transformer is negligible.

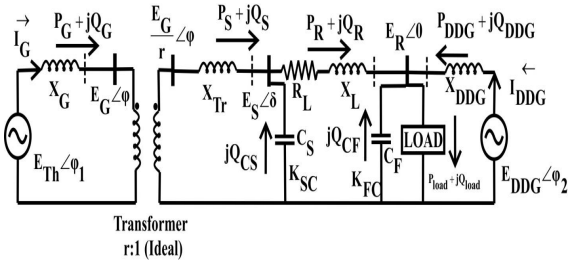

Fig.2. Equivalent circuit of fig.1.

The simplified equivalent circuit of Fig.1 is shown in Fig.2. the reactive power injected by capacitors can be written as:

$$Q_{CS} = K_{SC}\omega C_S E_S^2 \approx K_{SC} Q_{unitCS,rated} \quad (1)$$

$$Q_{CF} = K_{FC}\omega C_F E_R^2 \approx K_{FC} Q_{unitCF,rated} \quad (2)$$

Applying Kirchhoff's Current Law (K.C.L) at feeder input junction, the source current can be written as:

$$\tilde{I}_S = \tilde{I}_R - \tilde{I}_{QCS} = \left(\frac{P_R - jQ_R}{E_R}\right) - j\omega K_{SC} C_S E_S e^{j\delta} \quad (3)$$

$$\frac{\tilde{E_G}}{tap} = \tilde{E}_S + JX_{Tr}\tilde{I}_S = E_S e^{j\delta} + jX_{Tr}\left(\frac{P_R - jQ_R}{E_R}\right) + X_{Tr}\omega C_S E_S \quad (4)$$

After simplifications, the receiving end voltage and sending end voltages can be written as:

$$E_R = \sqrt{\frac{-\left(2(R_L P_R + X_L Q_R) - E_S^2\right) \pm \sqrt{\left(2(R_L P_R + X_L Q_R) - E_S^2\right)^2 - \left(4\left((R_L^2 + X_L^2)(P_R^2 + Q_R^2)\right)\right)}}{2}} \quad (5)$$

$$E_S = \sqrt{\left(\frac{1}{1+\left(\omega X_{Tr} k_S C_{CS}\right)}\right)^2 \left(\begin{array}{c}\left(\frac{E_G}{r}\right)^2 + \\ \left(\left(\frac{X_{Tr}}{E_R}\right)^2 \left(P_R^2 + Q_R^2\right)\right) \\ - \\ \left(2\frac{E_G}{r}\frac{X_{Tr}}{E_R}\left(\begin{array}{c} P_R \sin\varphi \\ + Q_R \cos\varphi \end{array}\right)\right)\end{array}\right)} \quad (6)$$

$$E_S = f_1(tap, K_{FC}, K_{SC}, Q_{DDG}) \quad (7)$$

$$E_R = f_2(tap, K_{FC}, K_{SC}, Q_{DDG}) \quad (8)$$

The equations show that the tap position of the ULTC, the number of capacitors connected to the feeder, the number of capacitors connected to the source end, and the reactive power injected by the DDG all influence the sending end voltage, receiving end voltage, and power loss of the feeder.

The objective function is formulated as:

$$J = \sum_{h=1}^{H-1} \left(\begin{array}{c} CP_{Loss} P_{Loss}^h \\ + C_{tap} |tap^{h+1} - tap^h| \\ + C_{SC} \left|k_{SC}^{h+1} - k_{SC}^h\right| \\ + \sum_{n=1}^{N} C_{FC} \left|k_{FCn}^{h+1} - k_{FCn}^h\right| \end{array} \right) \quad (9)$$

Where the control variables are defined as:

$$u_h = \left\{tap^h, k_B^h, k_{F1..N}^h, V_{DG1..S}^h\right\} \quad (10)$$

Subjected to the following constraints:

$$V_{min} \le V_b^h \le V_{max} \quad (11)$$

$$pf_{min} \le pf_{DGs}^h \le 1 \quad (12)$$

$$tap_{min} \le tap^h \le tap_{max} \quad (13)$$

$$0 \le K_{SC}^h \le K_{SC,max} \quad (14)$$

$$0 \le K_{FCn}^h \le K_{FCn,max} \quad (15)$$

h=1,2,3…….H, b=1,2,3…B and n=1,2……N.

III. REACTIVE POWER COORDINATION WITH PSO METHOD

Step 1: Generate initial positions of $X_i^0 X_i^0$ and respective velocities $Y_i^0 Y_i^0$ randomly, Load test system data

Generate initial positions of $X_i^0 X_i^0$ and respective velocities $Y_i^0 Y_i^0$ randomly for $i = 1,2,3 \dots \dots n. i = 1,2,3 \dots \dots n.$ forecast the load using ANFIS model and maximum number of iterations ($K_{max}) K_{max}$), Load test system data, i.e., is scheduled real power generation and maximum available reactive power of DDG and Load of the test system.

Step 2: Assume initial conditions that are required for power flow calculations

Assume bus voltage magnitudes equal to one and respective angles equal to zero, power loss equal to zero initially for all h, b, sh, b, s.

Step 3: Calculation of reactive power injected by the shunt capacitors

The reactive power injected by the shunt capacitors is calculated with the initial values specified in step 1 and step 3 using the equations (1) and (2) for all h, bh, b.

Step 4: Calculation of bus currents

Calculate the bus currents starting from the end buses of all branches to the slack bus of the main feeder using the equation (16).

$$I_b^h = \left(\frac{\left(S_{Lb}^h - S_{Dgs}^h\right)}{V_b^h}\right)^* + \sum_{m \in M} I_m^h \quad for\ all\ h, b, m$$

$$I_b^h = \left(\frac{\left(S_{Lb}^h - S_{Dgs}^h\right)}{V_b^h}\right)^* + \sum_{m \in M} I_m^h \quad for\ all\ h, b, m \quad (16)$$

Step 5: Check voltage mismatch condition

Determine the voltage mismatch using the equation (17) and check voltage mismatch using the equation (18); if satisfied, go to the next step; otherwise, go to step 3.

$$\left|\Delta\tilde{V}_b^{h,w}\right| = \left|\tilde{V}_b^{h,w}\right| - \left|\tilde{V}_b^{h,w-1}\right|$$
$$\left|\Delta\tilde{V}_b^{h,w}\right| = \left|\tilde{V}_b^{h,w}\right| - \left|\tilde{V}_b^{h,w-1}\right| \quad (17)$$

$$\left|\Delta\tilde{V}_b^{h,w}\right| < \varepsilon_b^h \left|\Delta\tilde{V}_b^{h,w}\right| < \varepsilon_b^h \quad (18)$$

Step 6: Check the DDG bus voltage mismatch condition

Determine the voltage mismatch at DDG buses using the equation (19) and check voltage mismatch using the equation (20); if satisfied, go to step 9; otherwise go to next step.

$$\left|\Delta V_{DDGs}^h\right| = \left|V_{DDGs,specified}^h\right| - \left|V_{DDGs,calculated}^h\right|$$
$$\left|\Delta V_{DDGs}^h\right| = \left|V_{DDGs,specified}^h\right| - \left|V_{DDGs,calculated}^h\right| \quad (19)$$

$$\left|\Delta V_{DDGs}^h\right| < \varepsilon_{DDGs}^h \left|\Delta V_{DDGs}^h\right| < \varepsilon_{DDGs}^h \quad (20)$$

Step 7: Update the DDG reactive power

Calculate the updated value of DDG reactive power using the equations (21) and (18).

$$\Delta Q_{DDGs}^h = H^{-1}\Delta V_{DDGs}^h \Delta Q_{DDGs}^h = H^{-1}\Delta V_{DDGs}^h \quad (21)$$

$$Q_{DDGs,new}^h = Q_{DDGs,old}^h + \Delta Q_{DDGs}^h$$
$$Q_{DDGs,new}^h = Q_{DDGs,old}^h + \Delta Q_{DDGs}^h \quad (22)$$

Where H is the sensitivity matrix

Step 8: Check the reactive power constraint of DDG

Check the reactive power of DDG updated in step 7 is within the limits or not using the equation (23). If satisfied, calculate the reactive power of DDG using equation (24); otherwise, calculate the reactive power of DDG using equation (25).

$$Q_{DDGs,min}^h \le Q_{DDGs,new}^h \le Q_{DDGs,max}^h$$
$$Q_{DDGs,min}^h \le Q_{DDGs,new}^h \le Q_{DDGs,max}^h \quad (23)$$

$$Q_{DDGs}^h = Q_{DDGs,new}^h Q_{DDGs}^h = Q_{DDGs,new}^h \quad (24)$$

$$Q_{DDGs}^h = max\left(min\left(Q_{DDGs,new}^h, Q_{DDGs,max}^h\right), Q_{DDGs,min}^h\right)$$
$$Q_{DDGs}^h = max\left(min\left(Q_{DDGs,new}^h, Q_{DDGs,max}^h\right), Q_{DDGs,min}^h\right) \quad (25)$$

Step 9: Stop the power flow calculation and return the real power loss of distribution system, voltage magnitudes of buses and calculated voltages of DDGs.

Step 10: Adjustment of initial positions of $X_i^0 X_i^0$

Initial values of $X_i^0 X_i^0$ are adjusted to meet the voltage constraint represented in equation (26).

$$V_{min} \le V_b^h \le V_{max} V_{min} \le V_b^h \le V_{max} \quad (26)$$

Step 11: Calculation of fitness function and update $P_i^k P_i^k$ and $G^k G^k$

Calculate the fitness function using the equation (27) and update $P_i^k P_i^k$ and $G^k G^k$ with adjusted values of $X_i^0 X_i^0$.

$$J = \sum_{h=1}^{H-1}\left(CP_{Loss}P_{Loss}^h + C_{tap}\left|tap^{h+1} - tap^h\right| + C_{SC}\left|k_{SC}^{h+1} + \sum_{n=1}^{N} C_{FC}\left|k_{FCn}^{h+1} - k_{FCn}^h\right|\right.$$
$$J = \sum_{h=1}^{H-1}\left(CP_{Loss}P_{Loss}^h + C_{tap}\left|tap^{h+1} - tap^h\right| + C_{SC}\left|k_{SC}^{h+1} - k_{SC}^h\right| + \sum_{n=1}^{N} C_{FC}\left|k_{FCn}^{h+1} - k_{FCn}^h\right|\right) \quad (27)$$

Step 12: Update $X_i^k X_i^k$ and $P_i^k P_i^k$

After the evolution of fitness function then update the values of $X_i^k X_i^k$ and $P_i^k P_i^k$ using the equations (28) to (30).

$$Y_i^{k+1} = \begin{pmatrix} round\left(w \cdot Y_i^k\right) + round\left(c_1 \cdot rn(0,1) \cdot \left(P_i^k - X_i^k\right)\right) + \\ round\left(c_2 \cdot rn(0,1) \cdot \left(G^k - X_i^k\right)\right) \end{pmatrix} \quad (28)$$

$$w = w_{max} - \left(w_{max} - w_{min}\right) \times \frac{k}{k_{max}} \quad (29)$$

$$X_i^{k+1} = X_i^k + Y_i^k \quad (30)$$

Step 13: Calculation of reactive power injected by the shunt capacitors

The reactive power injected by the shunt capacitors is calculated with the updated values obtained from step 12 for all h, bh, b.

Step 14: Calculation of bus currents

Calculate the bus currents starting from the end buses of all branches to the slack bus of the main feeder using the equation (31).

$$I_b^h = \left(\frac{\left(s_{Lb}^h - s_{Dgs}^h\right)}{V_b^h}\right)^* + \sum_{m \in M} I_m^h \quad for\ all\ h, b, m$$
$$I_b^h = \left(\frac{\left(s_{Lb}^h - s_{Dgs}^h\right)}{V_b^h}\right)^* + \sum_{m \in M} I_m^h \quad for\ all\ h, b, m \quad (31)$$

Step 15: Check voltage mismatch condition

Determine the voltage mismatch using the equation (19) and check voltage mismatch using the equation (20); if satisfied, go to the next step; otherwise, go to step 13.

Step 16: Check the DDG bus voltage mismatch condition

Determine the voltage mismatch at DDG buses using the equation (15) and check voltage mismatch using the equation (16); if satisfied, go to step 21; otherwise go to next step.

Step 17: Update the DDG reactive power

Calculate the updated value of DDG reactive power using the equations (21) and (22).

Step 18: Check the reactive power constraint of DDG

Check the reactive power of DDG updated in step 17 is within the limits or not using the equation (23). If satisfied, calculate the reactive power of DDG using equation (24); otherwise, calculate the reactive power of DDG using equation (25).

Step 19: Stop the power flow calculation, and return the real power loss of the distribution system, voltage magnitudes of buses, and calculated voltages of DDGs.

Step 20: Check the fitness function condition and iteration condition

Check the fitness function is satisfied or not using the equation (32) and check iterations equal to maximum

number of iterations using the equation (33). If these two conditions are satisfying then stop the procedure and return power loss, voltages at all buses and reactive power supplied or absorbed by DDG. Otherwise, increase iteration by one and then repeat steps from 11 to 20.

$$J^K - J^{K-1} < \varepsilon \quad (32)$$

$$K \geq K_{max} \quad (33)$$

Step 21: Calculation of Steady-State Voltage Fluctuations (SSVF)

Calculate SSVF using the equation (below) with the voltages updated in step 20.

$$SSVF = \frac{1}{B}\sum_{b=1}^{B}\left(\sum_{h=1}^{H-1}\left|V_b^{h+1} - V_b^h\right|\right) \quad for\ all\ values\ of\ b,h$$

V. CASE STUDY & RESULTS

Fig.5 shows the active power PL for total loads forecasted one day in advance in the three distribution feeders. Feeder 3 has a considerably different profile from feeders 1 and 2; with the smallest difference between the maximum and minimum loads. Fig.5 represents the total load demands, ranging from 8.8 to 32.5 MW, in the test grid. Rapid load variation from h = 11–13 is often observed, especially in small-scale grids where residential or industrial loads make up a significant portion. Furthermore, assume that PDDG is pre-dispatched to one of three different profiles as shown in Fig.3 & 4 to meet the load demand with the active power supplied from the transmission network. The profiles have the same average value of 2 MW (for 2MW DDG) & 3 MW (for 3MW DDG), which implies that the DDGs have the same average reactive power available for coordination with the ULTC and SCs for all the PDDG profiles.

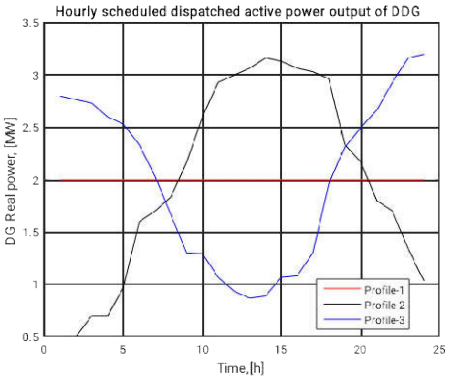

Fig.3. Output patterns of 2MW DDG

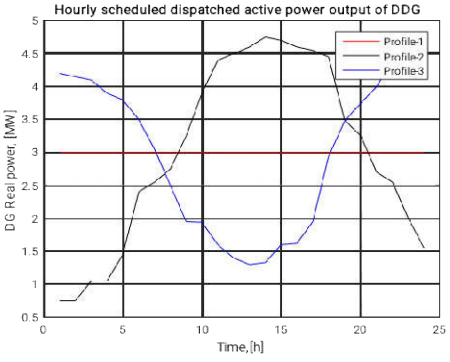

Fig.4. Output patterns of 3MW DDG

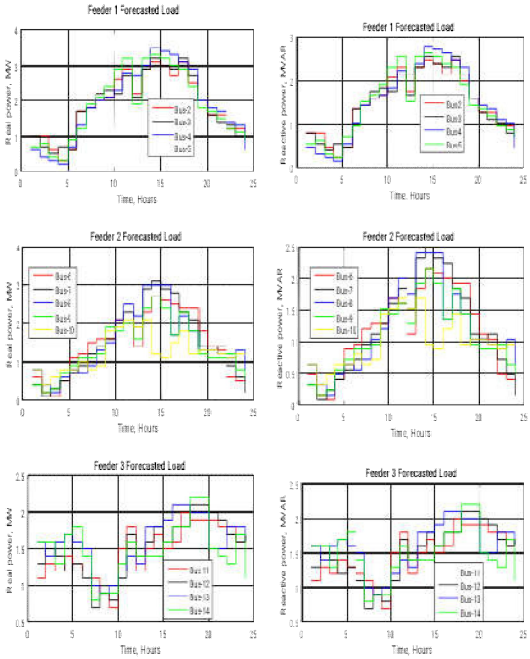

Fig.5. Forecasted loads of feeders using ANFIS

After determining the optimal dispatch schedules of the DDG and switching devices in both the conventional and proposed control methods, with $CP_{Loss}: C_{tap}: C_{SC}: C_{FC} CP_{Loss}: C_{tap}: C_{SC}: C_{FC}$ set equal to 80$:80$:60$:40$, the total power loss, power quality and Switching Operation Number (SON) of the ULTC and SCs were evaluated and compared.

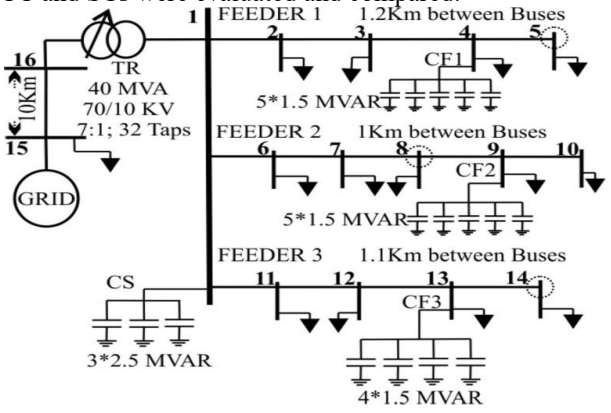

Fig.6. Grid-connected 10kV practical system single line diagram.

Table 1.power loss, switching loss of ULTC & SCs, Total loss and SSVF are the performance parameters for the comparison of proposed methods.

Table.1 3MW DDG located at bus 5 (profile 1) & 2MW DDG located at bus 8 (profile 1)

Control Methods		Conventional Method	PSO Method
Power loss (MWh)		8.81147	8.79133
SSVF(%)		0.303805	0.245472
	ULTC	7	2

SONs of VCDs	SC	2	3
	FC1	11	8
	FC2	9	5
	FC3	9	1
Power loss ($)		704.9176	703.3064
Switching loss ($)		1840	900
Total loss ($)		2544.9176	1603.3064

Table 1 shows the simulation results and performance comparison of conventional and PSO methods, when 3MW DDG connected to bus 5 on feeder 1 with output profile 1 and 2MW DDG connected to bus 8 on feeder 2 with output profile 1. SSVF, power loss, switching loss and total loss were reduced by the reactive power support of 3MW DDG & 2MW DDG, illustrated in Table 1.

The simulation results and performance comparison of conventional, PSO and GWO methods, when 3MW DDG connected to bus 5 on feeder 1 with output profile 1 and 2MW DDG connected to bus 8 on feeder 2 with output profile 2 is shown in Table 2. As illustrated in Table 2, the reactive power support of 3MW DDG & 2MW DDG reduced the SSVF, power loss, switching loss and total loss.

Table.2 3MW DDG located at bus 5 (profile 1) & 2MW DDG located at bus 8 (profile 2)

Control Methods		Conventional Method	PSO Method
Power loss (MWh)		9.75303	9.7377
SSVF(%)		0.250341	0.250011
SONs of VCDs	ULTC	6	2
	SC	2	3
	FC1	11	9
	FC2	7	6
	FC3	7	6
Power loss ($)		780.2424	779.016
Switching loss ($)		1600	1180
Total loss ($)		2380.2424	1959.016

Table.3 3MW DDG located at bus 5 (profile 1) & 2MW DDG located at bus 8 (profile 3)

Control Methods	Conventional Method	PSO Method
Power loss (MWh)	8.50579	8.21779
SSVF(%)	0.256288	0.256184
SONs of VCDs	ULTC	6	2
	SC	2	3
	FC1	11	6
	FC2	7	6
	FC3	7	11
Power loss ($)		680.4632	657.4232
Switching loss ($)		1600	1260
Total loss ($)		2280.4632	1917.4232

Table 3 shows the simulation results and performance comparison of conventional and PSO methods, when 3MW DDG connected to bus 5 on feeder 1 with output profile 1 and 2MW DDG connected to bus 8 on feeder 2 with output profile 3. SSVF, power loss, switching loss and total loss were reduced by the reactive power support of 3MW DDG & 2MW DDG, illustrated in Table 3.

The simulation results and performance comparison of conventional and PSO methods,, when 3MW DDG connected to bus 5 on feeder 1 with output profile 2 and 2MW DDG connected to bus 8 on feeder 2 with output profile 1 is shown in Table 4. As illustrated in Table 4, the reactive power support of 3MW DDG & 2MW DDG reduced the SSVF, power loss, switching loss and total loss.

Table.4 3MW DDG located at bus 5 (profile 2) & 2MW DDG located at bus 8 (profile 1)

Control Methods		Conventional Method	PSO Method
Power loss (MWh)		10.2766	9.5232
SSVF(%)		0.3092	0.264597
SONs of VCDs	ULTC	6	3
	SC	1	0
	FC1	11	11
	FC2	10	4
	FC3	7	15
Power loss ($)		822.128	761.856
Switching loss ($)		1660	1440
Total loss ($)		2482.128	2201.856

Table.5 3MW DDG located at bus 5 (profile 2) & 2MW DDG located at bus 8 (profile 2)

Control Methods		Conventional Method	PSO Method
Power loss (MWh)		11.639	10.3822
SSVF(%)		0.326836	0.323521
SONs of VCDs	ULTC	7	4
	SC	1	8
	FC1	11	7
	FC2	7	4
	FC3	5	2
Power loss ($)		931.12	830.576
Switching loss ($)		1540	1320
Total loss ($)		2471.12	2150.576

Table 5 shows the simulation results and performance comparison of conventional and PSO methods, when 3MW DDG connected to bus 5 on feeder 1 with output profile 2 and 2MW DDG connected to bus 8 on feeder 2 with output profile 2. SSVF, power loss, switching loss and total loss were reduced by the reactive power support of 3MW DDG & 2MW DDG, illustrated in Table 5.

Table 6 shows the simulation results and performance comparison of conventional and PSO methods, when 3MW DDG connected to bus 5 on feeder 1 with output profile 2 and 2MW DDG connected to bus 8 on feeder 2 with output profile 3. SSVF, power loss, switching loss and total loss were reduced by the reactive power support of 3MW DDG & 2MW DDG, illustrated in Table 6.

Table.6 3MW DDG located at bus 5 (profile 2) & 2MW DDG located at bus 8 (profile 3)

Control Methods		Conventional Method	PSO Method
Power loss (MWh)		9.73503	9.5739
SSVF(%)		0.269238	0.251904
SONs of VCDs	ULTC	5	0
	SC	1	1
	FC1	11	7
	FC2	12	5
	FC3	9	14
Power loss ($)		778.8024	765.912
Switching loss ($)		1740	1100
Total loss ($)		2518.8024	1865.912

Table.7 3MW DDG located at bus 5 (profile 3) & 2MW DDG located at bus 8 (profile 1)

Control Methods		Conventional Method	PSO Method
Power loss (MWh)		7.74697	7.64597
SSVF(%)		0.298363	0.25258
SONs of VCDs	ULTC	8	4
	SC	1	4
	FC1	14	9
	FC2	13	6
	FC3	5	1
Power loss ($)		619.7576	611.6776
Switching loss ($)		1980	1200
Total loss ($)		2599.7576	1811.6776

Table.8 3MW DDG located at bus 5 (profile 2) & 2MW DDG located at bus 8 (profile 3)

Control Methods		Conventional Method	PSO Method
Power loss (MWh)		8.48351	7.6943
SSVF(%)		0.270614	0.266173
SONs of VCDs	ULTC	7	2
	SC	1	9
	FC1	14	11
	FC2	13	6
	FC3	5	4
Power loss ($)		678.6808	615.544
Switching loss ($)		1900	1540
Total loss ($)		2578.6808	2155.544

Table.9 3MW DDG located at bus 5 (profile 3) & 2MW DDG located at bus 8 (profile 3)

Control Methods	Conventional Method	PSO Method
Power loss (MWh)	7.56061	7.5115
SSVF(%)	0.303211	0.289314

SONs of VCDs	ULTC	8	2
	SC	1	10
	FC1	14	6
	FC2	13	6
	FC3	5	2
Power loss ($)		604.8488	600.92
Switching loss ($)		1980	1320
Total loss ($)		2584.8488	1920.92

Table 7 shows the simulation results and performance comparison of conventional and PSO methods, when 3MW DDG connected to bus 5 on feeder 1 with output profile 3 and 2MW DDG connected to bus 8 on feeder 2 with output profile 1. SSVF, power loss, switching loss and total loss were reduced by the reactive power support of 3MW DDG & 2MW DDG, illustrated in Table 7.

The simulation results and performance comparison of conventional and PSO methods, when 3MW DDG connected to bus 5 on feeder 1 with output profile 3 and 2MW DDG connected to bus 8 on feeder 2 with output profile 2 is shown in Table 8. As illustrated in Table 8, the reactive power support of 3MW DDG & 2MW DDG reduced the SSVF, power loss, switching loss and total loss.

Table 9 shows the simulation results and performance comparison of conventional and PSO methods, when 3MW DDG connected to bus 5 on feeder 1 with output profile 3 and 2MW DDG connected to bus 8 on feeder 2 with output profile 3. SSVF, power loss, switching loss and total loss were reduced by the reactive power support of 3MW DDG & 2MW DDG, illustrated in Table 9.

VI. CONCLUSIONS

This paper proposes a novel method, which includes load forecasting and scheduling of switching operations of ULTC & SCs. The proposed method is implemented in MATLAB/Simulink on 10kV 16 bus system and performance is compared with conventional method. From the findings, it is clear that the proposed method is effectively reducing the objectives as compared with conventional method.

References

[1] Keane, A., Ochoa, L. F., Borges, C. L. T., et al.: 'State-of-the-art techniques and challenges ahead for distributed generation planning and optimization', IEEE Trans. Power Syst., 2013, 28, (2), pp.1493-1502.

[2] Rueda-Medina, A. C., Padilha-Feltrin, A.: 'Distributed generators as providers of reactive power support-a market approach', IEEE Trans. Power Syst., 2013, 28, (1), pp.490-502.

[3] Viawan, F. A., Karlsson, D.: 'Combined local and remote voltage and reactive power control in the presence of induction machine distributed generation', IEEE Trans. Power Syst., 2007, 22, (4), pp.2003-2012.

[4] Viawan, F. A., Karlsson, D.: 'Voltage and reactive power control in systems with synchronous machine based distributed generation', IEEE Trans. Power Del., 2008, 23, (2), pp.1079-1087.

[5] Dent, C. J., Ochoa, F. F., Harrison, G. P.: 'Network distributed generation capacity analysis using OPF with voltage step constraints', IEEE Trans. Power Syst., 2010, 25, (1), pp.296-304.

[6] Ahmadi, A. R., Green, T. C.: 'Optimal power flow for autonomous regional active network management system', IEEE Power & Energy Society General Meeting, 2009, pp.1-7.

[7] Kim, Y. J., Ahn, S. J., Hwang, P. I., et al.: 'Combined control of a DG and voltage control devices using a dynamic programming algorithm', IEEE Trans. Power Syst., 2013, 28, (1), pp.42-51.

[8] Tanaka, K., Oshiro, M., Toma, S., et al.: 'Decentralised control of voltage in distribution systems by distributed generators', IET Gener., Transm&Distrib., 2010, 4, (11), pp.1251-1260.

[9] Sankaraiah, M., Suresh Reddy, S., Vijaya Kumar, M.: 'Particle swarm optimization based reactive power coordinated control of distributed generation and voltage controlled devices', The Journal of CPRI, 2017, 13, (3), pp.447-454.

[10] Sheng, W., Liu, K. Y., Ye, X., et al.: 'A reactive power coordinated optimization method with renewable distributed generation based on Improved harmony search', IET Gener. Trans &Distrib., 2016, 10, (13), pp.3152-3162.

[11] Sankaraiah, M., Suresh Reddy, S., Vijaya Kumar, M.: 'GWO Based optimal reactive power coordination of DFIG, ULTC & Capacitors', Indonesian J ElecEng& Comp Sci, 2018, 11, (3), pp.805-813.

[12] M. Sankaraiah, S. Suresh Reddy, M. Vijaya Kumar, "Optimized Reactive Power Coordination of Distributed Generation and Voltage Controlled Devices Based on GWO", Journal of Mechanics of Continua and Mathematical Sciences, No.5, pp. 283-307, 2020 (January).

[13] M. Sankaraiah, S. Suresh Reddy, M. Vijaya Kumar, "PSO Based Reactive Power Coordination of Multiple Dispatchable Distributed Generations & Voltage Controlled Devices", International Journal of Innovative Technology and Exploring Engineering, Vol. 8, No. 10, pp. 1308-1313, 2019.

[14] M. Sankaraiah, S. Suresh Reddy, M. Vijaya Kumar, "DFIG and voltage controlled devices reactive power coordination using particle swarm optimization", IEEE International Conference for Convergence in Technology, Manglore, India, Oct 2018. 2.

[15] M. Sankaraiah, S. Suresh Reddy, M. Vijaya Kumar, "PSO based reactive power coordination of PV system and voltage controlled devices", Third International Conference on Emerging Trends in Electrical, Communications and Information Technology (Springer conference), Ananthapuramu, India, Dec 2018.

[16] T. Senjyu, H. Takara, K. Uezato and T. Funabashi, "One-Hour-Ahead Load Forecasting Using Neural Network", IEEE Transaction on Power Systems, vol. 17, no.1, February 2002.